Identification and simulation of the $H_2{}^{16}O$ absorption spectrum in 5750–7965 cm^{-1} region

A.D. Bykov, O.V. Naumenko, A.P. Shcherbakov, L.N. Sinitsa, and B.A. Voronin

Institute of Atmospheric Optics,
Siberian Branch of the Russian Academy of Sciences, Tomsk

Received September 13, 2004

The rotational, centrifugal distortion, and resonance coupling constants as well as dipole moment parameters of six vibrational states, *viz.*, (101), (021), (120), (200), (002), and (040) of the $H_2{}^{16}O$ molecule have been determined from the fit to the experimental rotational energy levels and line strengths measured by R.A. Toth [Appl. Opt. **33**, 4851(1994)]. Quite satisfactory agreement for the energy levels and intensities have been achieved using the effective rotational Hamiltonian in the Padé–Borel form and taking into account the conventional Coriolis, Fermi, Darling–Dennison, and the high-order resonance couplings. The rms deviation of the fitting is 0.025 cm^{-1} and 4.86% for 858 energy levels and intensities of 3038 lines, respectively. The calculations made enabled complete assignment of the lines of the experimental spectrum.

Introduction

The most detailed and accurate absorption spectrum of water vapor in the 5750–7965 cm^{-1} region, interesting for various applications, was recorded in Ref. 1. In Ref. 2, the H_2O absorption spectrum was experimentally recorded and theoretically analyzed in a rather narrow spectral range of 6380–6600 cm^{-1}, corresponding to an atmospheric transmission window. The use of high-sensitivity CRDS (Cavity Ring Down Spectroscopy) technique in Ref. 2 significantly increased the number of H_2O absorption lines (2270 in place of 925), recorded in the region under study. The spectrum recorded in Ref. 2 was assigned with the use of the precision Partridge and Schwenke calculation of the water vapor absorption spectrum.[3] It was shown in Ref. 2 that in the 5750–7965 cm^{-1} region the HITRAN databank of spectroscopic information contains, along with the data from Ref. 1, many lines with bad mistakes in the line positions and intensities, which originate from the old version of HITRAN.

In Ref. 4, the experimental energy levels from Ref. 1 were modeled with high accuracy (0.014 cm^{-1}) based on the new theoretical model of the effective Hamiltonian – method of generating functions. Some experimental levels from Ref. 1 were excluded from the analysis in Ref. 4, because they deviated far from the calculation and thus were assumed errors. Note that the intensity of H_2O RV lines was not modeled in Ref. 4, and this restricts the applicability of these results to more accurate assignment of the spectrum recorded in Ref. 1.

In this paper, we perform new assignment and modeling of the H_2O absorption spectrum near 1.4 μm for the following reasons. The analysis reported in Ref. 1 and earlier papers was mostly based on the method of combination differences, and the assignment of weak lines with high values of the rotational quantum number J raises some doubts, because it was not based on the precision calculations of line positions and intensities. Moreover, some of the recorded lines remained unassigned.

In contrast to previous investigations, in this work the assignment was performed by iterations with the use of the Expert system for automatic assignment of rovibrational spectra.[5] First, the parameters of the Hamiltonian and dipole moment were fitted to the initial set of experimental positions and intensities of lines with the low values of the rotational quantum number J. At the next stage, weak lines, corresponding to the higher values of the quantum number J were assigned based on the calculations with the use of the fitted parameters, combination differences, and the data of the Partridge and Schwenke calculation.[3] Finally, the energy levels determined from the spectrum were included in the fitting to refine the spectroscopic constants, and the assignment procedure was repeated.

1. Assignment of H_2O spectrum and determination of the experimental energy levels

The assignment of strong lines in the spectrum used the data from Ref. 1 and was applied to training the assignment program.[5] The positions and intensities of these lines served the initial information for refinement of rotational, centrifugal distortion, and resonance coupling constants, as well as parameters of the effective dipole moment operator. The further work, involving the assignment of weak lines, was carried out step by step with the fitting of spectroscopic constants at every new step and the predictive calculations. Along with the calculation by the effective Hamiltonian method, the synthetic

0235-6880/04/12 940-08 $02.00

spectrum from Ref. 3 was used in the assignment. The experimental energy levels were determined by averaging over all lines of a combination difference with the use of rotational levels of the ground vibrational states from Ref. 6.

As a result, 97% of 4097 experimental lines recorded in Ref. 1 were assigned; some of unassigned lines may be, in our opinion, artifacts. The assignment of many lines with high J was incorrect in Ref. 1, and these lines were re-assigned in accordance with our calculations of line positions and intensities (see below). The resultant list of experimental line positions and intensities, their quantum assignment, and intensities calculated in this work is attached to the publication in the electronic format and can be accessed by a request.

A total of 866 high-accuracy energy levels were determined for the states (101), (021), (120), (200), (002), (040), and (050) of the $H_2{}^{16}O$ molecule, whereas in Ref. 1 the number of determined energy levels was only 673, and some of them were incorrect. We have re-assigned some experimental levels from Ref. 1 based on the analysis of mixing coefficients of wave functions. The comparison of the obtained array of experimental levels with the most complete compilation[7] showed that 56 of them are absent in Ref. 7. These levels are summarized in Table 1. However, some of these levels were also obtained by Macko with co-authors,[2] who studied this problem in parallel with us. The energy levels reported in Ref. 2 are marked by asterisk in Table 1. Thus, our assignment yielded 29 new energy levels for the first hexade of the $H_2{}^{16}O$ molecule.

2. Simulation of RV energy levels of the $H_2{}^{16}O$ molecule

The experimental energy levels were simulated using the effective Hamiltonian in the form

$$H = \begin{vmatrix} W_{101} & & & & & \\ F_{021-101} & W_{021} & & & \mathrm{HC} & \\ C_{120-101} & C_{120-021} & W_{120} & & & \\ C_{200-101} & C_{200-021} & F_{200-120} & W_{200} & & \\ C_{002-101} & 0 & F_{002-120} & F_{002-200} & W_{002} & \\ 0 & C_{040-021} & F_{040-120} & F_{040-200} & 0 & W_{040} \end{vmatrix}, \quad (1)$$

where W_V are the diagonal operators, corresponding to the vibrational state V, and $F_{VV'}$ and $C_{VV'}$ are the resonance operators, accounting for the anharmonic resonances (F) or Coriolis coupling (C); HC denotes Hermitian conjugation. Because of the presence of strong bending–rotational interaction in the vibrational state (040), the effective rotational Hamiltonian for all the states was represented with the use of Padé–Borel approximants.[8]

Table 1. Novel energy levels of the $H_2{}^{16}O$ molecule for the states (101), (021) and (120), (200) and (002), in cm^{-1}

V_1	V_2	V_3	J	K_a	K_c	$E_{exp.}$	Δ	N	V_1	V_2	V_3	J	K_a	K_c	E_{exp}	Δ	N
1	0	1	9	9	1	9314.8221	1.37	2	2	0	0	9	7	3	8935.2713 *	0.12	1
1	0	1	9	9	0	9314.8223	1.64	2	2	0	0	10	3	7	8686.9806	0.02	2
1	0	1	10	10	1	9783.1683		1	2	0	0	10	9	2	9547.6587		1
1	0	1	10	10	0	9783.1683		1	2	0	0	10	9	1	9547.6586 *		1
1	0	1	11	8	4	9667.0392		1	2	0	0	11	3	9	8834.4081 *	0.03	2
1	0	1	11	8	3	9666.9665		1	2	0	0	11	4	8	8975.0935 *	1.05	2
1	0	1	12	8	4	9953.6164 *		1	2	0	0	11	5	7	9119.8039 *	0.27	2
1	0	1	13	5	8	9778.8804		1	2	0	0	12	4	8	9329.6872 *		1
1	0	1	13	6	7	9894.5338	1.58	2	2	0	0	12	6	6	9548.1381 *		1
1	0	1	13	6	7	10046.9859		1	2	0	0	13	2	11	9368.7979 *		1
1	0	1	14	3	12	9710.5013		1	2	0	0	13	3	10	9532.8738		1
1	0	1	17	1	16	10424.0090		1	2	0	0	13	5	9	9684.6367 *	0.39	2
0	2	1	11	8	3	9598.7785		1	2	0	0	14	1	13	9442.3237 *		1
0	2	1	12	8	5	9885.1049		1	0	0	2	9	3	7	8614.3414 *	0.16	3
1	2	0	9	5	4	8373.9664		1	0	0	2	9	8	2	9328.5834	0.37	3
1	2	0	9	8	2	9059.1429 *	2.16	2	0	0	2	9	8	1	9328.5832	0.50	3
1	2	0	9	8	1	9059.1449	0.38	2	0	0	2	10	5	5	9103.3016 *		1
1	2	0	10	2	9	8081.6684 *	0.04	3	0	0	2	10	7	3	9377.1131		1
1	2	0	10	2	8	8241.5177 *		1	0	0	2	10	8	2	9571.3731		1
1	2	0	10	5	5	8615.5096 *		1	0	0	2	10	10	1	9960.8561		1
1	2	0	11	2	10	8311.9493 *		1	0	0	2	10	10	0	9960.8561		1
1	2	0	11	3	9	8507.1464 *		1	0	0	2	11	5	7	9355.8605	2.28	2
1	2	0	11	5	7	8876.1984 *	0.40	3	0	0	2	11	6	6	9497.9798 *	0.41	2
1	2	0	12	0	12	8291.1775 *	0.26	2	0	0	2	11	8	4	9836.3654 *		1
1	2	0	12	2	10	8770.1057 *		1	0	0	2	11	8	3	9836.3420 *		1
1	2	0	12	4	9	8969.9465 *	0.69	2	0	0	2	12	6	6	9789.5646		1
1	2	0	13	3	10	9239.7643 *		1	0	0	2	13	4	10	9796.1809		1
1	2	0	14	4	10	9702.1947		1	0	0	2	15	1	15	9728.4144		1

Note. N is the number of lines, from which the level was determined; Δ is the rms error of determination of the energy level, in $10^{-3} \cdot cm^{-1}$.

The resonance operators were represented in the form

$$F = F_0 + F_k J_z^2 + F_J J^2 + F_{xy} J_{xy}^2 + F_{xyk}\{J_z^2, J_{xy}^2\} \quad (2)$$

for anharmonic resonances and

$$C = C_y i J_y + C_{xz}\{J_x, J_z\} + C_{xzk}\{J_z^{\,3}, J_x\}_+ + \\ + C_{xzJ}\{J_x, J_z\}_+ J^2 + C_{xzkJ}\{J_x, J_z^3\}_+ J^2 \quad (3)$$

for the Coriolis coupling with all the designations corresponding to the commonly accepted ones. It should be noted that we used the model, in which all parameters F_0 were taken zero. This decreases the number of Hamiltonian parameters to be determined from the fitting, but it should be kept in mind that the rotational and centrifugal distortion parameters obtained in this case are a superposition of the constants of the effective Hamiltonian, written in the standard form.

The proper choice of the initial approximation for spectroscopic parameters is important for the correct solution of the inverse problem. Thus, the rotational and centrifugal distortion constants of vibrational states, having the same quantum numbers of the bending vibration V_2, should be close, because the water molecule is characterized by the strong dependence on V_2 and the weak dependence on the quantum numbers V_1 and V_3, corresponding to the stretching vibrations. Therefore, in the initial approximation, all high-order centrifugal parameters were fixed to the values for the lower states with the same quantum number V_2. For the vibrational states (101), (200), and (002), the fixed centrifugal constants were taken equal to the same parameters of the vibrational state (001), and for the vibrational states (120) and (021) they were taken as in the state (020). For the high-excited bending state (040), the high-order centrifugal parameters were extrapolated from the corresponding parameters of the state (030). In the process of fitting, some of the fixed parameters were refined.

All, except five, energy levels determined from the experiment for the first hexade were included in the fitting: a total of 858 experimental energy levels and 120 fitting parameters were used, and the results obtained appeared to be in a good agreement with the experimental data, which allowed the reliable and unambiguous assignment of the spectrum analyzed. The standard deviation was 0.025 cm^{-1}. The resultant vibrational energies, rotational, centrifugal distortion, and resonance constants for the second hexade of $H_2{}^{16}O$ molecule are presented in Tables 2 and 3 along with the 68% confidence intervals. The fixed parameters are presented in Table 2 without confidence intervals.

Table 2. Vibrational energies, rotational and centrifugal distortion constants of the states (101), (200), (002), (021), (120), and (040) of the $H_2{}^{16}O$ molecule, in cm^{-1}

Parameter	(101)	(200)	(002)
E_v	7249.8184	7201.5402	7445.0453
A	25.975426(920)	26.36054(150)	25.61023(105)
B	14.217436(460)	14.120262(450)	14.306525(552)
C	8.958816(380)	8.931531(200)	8.990924(553)
Δ_k	$0.274761(510)\cdot 10^{-1}$	$0.28419(120)\cdot 10^{-1}$	$0.2647(579)\cdot 10^{-1}$
Δ_{Jk}	$-0.55023(190)\cdot 10^{-2}$	$-0.52322(280)\cdot 10^{-2}$	$-0.58415(278)\cdot 10^{-2}$
Δ_J	$1.303318(870)\cdot 10^{-3}$	$1.210024(820)\cdot 10^{-3}$	$1.384399(949)\cdot 10^{-3}$
δ_k	$0.11824(150)\cdot 10^{-2}$	$0.13006(230)\cdot 10^{-2}$	$0.11232(223)\cdot 10^{-2}$
δ_J	$0.53367(180)\cdot 10^{-3}$	$0.49476(114)\cdot 10^{-3}$	$0.56075(319)\cdot 10^{-3}$
H_k	$0.94987(890)\cdot 10^{-4}$	$0.10226(301)\cdot 10^{-3}$	$0.8435(119)\cdot 10^{-4}$
H_{kJ}	$-0.12264(570)\cdot 10^{-4}$	$-0.1471(103)\cdot 10^{-4}$	$-0.12860(812)\cdot 10^{-4}$
H_{Jk}	$-0.1353(120)\cdot 10^{-5}$	$-0.1570(194)\cdot 10^{-5}$	$-0.1574(202)\cdot 10^{-5}$
H_J	$0.66\cdot 10^{-6}$	$0.66\cdot 10^{-6}$	$0.66\cdot 10^{-6}$
h_k	$0.26696(860)\cdot 10^{-4}$	$0.2923(167)\cdot 10^{-4}$	$0.2322(161)\cdot 10^{-4}$
h_J	$0.36080(680)3\cdot 10^{-6}$	$0.33\cdot 10^{-6}$	$0.3429(133)\cdot 10^{-6}$
L_k	$-0.12\cdot 10^{-6}$	$-0.12\cdot 10^{-6}$	$-0.12\cdot 10^{-6}$
L_{kJ}	$0.12\cdot 10^{-6}$	$0.12\cdot 10^{-6}$	$0.12\cdot 10^{-6}$
L_{kJk}	$-0.57\cdot 10^{-7}$	$-0.57\cdot 10^{-7}$	$-0.57\cdot 10^{-7}$
Parameter	(021)	(120)	(040)
E_v	6871.5204	6775.0928	6134.0148
A	33.370411(730)	34.47499(130)	52.62502(190)
B	14.786629(610)	14.642307(860)	15.13455(102)
C	8.843220(530)	8.794248(800)	8.630623(761)
Δ_k	$0.937154(580)\cdot 10^{-1}$	0.106243(170)	0.723935(186)
Δ_{Jk}	$-0.104585(400)\cdot 10^{-1}$	$-0.110277(460)\cdot 10^{-1}$	$-0.233831(576)\cdot 10^{-1}$
Δ_J	$0.168605(230)\cdot 10^{-2}$	$1.630307(930)\cdot 10^{-3}$	$0.21435(100)\cdot 10^{-2}$
δ_k	$0.85431(590)\cdot 10^{-2}$	$0.8740(100)\cdot 10^{-2}$	$0.63135(157)\cdot 10^{-1}$
δ_J	$0.67912(340)\cdot 10^{-3}$	$0.69307(920)\cdot 10^{-3}$	$0.92132(833)\cdot 10^{-3}$
H_k	$0.99361(510)\cdot 10^{-3}$	$0.13309(120)\cdot 10^{-2}$	$0.40\cdot 10^{-1}$
H_{kJ}	$-0.9927(330)\cdot 10^{-4}$	$-0.15849(290)\cdot 10^{-3}$	$-0.82638(782)\cdot 10^{-3}$
H_{Jk}	$0.60\cdot 10^{-5}$	$0.7216(440)\cdot 10^{-5}$	$0.11578(147)\cdot 10^{-3}$
H_J	$0.183658(690)\cdot 10^{-5}$	$0.15\cdot 10^{-5}$	$0.42024(300)\cdot 10^{-5}$

Table 2 (Continued)

Parameter	(021)	(120)	(040)
h_k	$0.27772(900) \cdot 10^{-3}$	$0.2704(150) \cdot 10^{-3}$	$0.75 \cdot 10^{-2}$
h_{Jk}	$0.9506(380) \cdot 10^{-5}$	$0.684(100) \cdot 10^{-5}$	0.00
h_J	$0.3710(140) \cdot 10^{-6}$	$0.8462(630) \cdot 10^{-6}$	$0.12026(657) \cdot 10^{-5}$
L_k	$-0.17572(540) \cdot 10^{-5}$	$-0.2142(120) \cdot 10^{-5}$	$-0.233452(309) \cdot 10^{-3}$
L_{kJ}	$0.9400(390) \cdot 10^{-6}$	$0.13 \cdot 10^{-5}$	$0.11109(200) \cdot 10^{-4}$
L_{kJk}	$-0.63140(830) \cdot 10^{-6}$	$-0.64 \cdot 10^{-6}$	$-0.60 \cdot 10^{-5}$
L_{Jk}	$0.65 \cdot 10^{-7}$	$0.65 \cdot 10^{-7}$	0.00
L_J	$-0.24 \cdot 10^{-8}$	$-0.24 \cdot 10^{-8}$	0.00
l_k	$0.5627(130) \cdot 10^{-5}$	$0.64 \cdot 10^{-5}$	$0.155025(471) \cdot 10^{-3}$
l_{kJ}	$-0.44 \cdot 10^{-6}$	$-0.3058(700) \cdot 10^{-6}$	$-0.80 \cdot 10^{-6}$
P_k	$0.29 \cdot 10^{-8}$	$0.29 \cdot 10^{-8}$	$0.16 \cdot 10^{-5}$

Note. 68% confidence intervals in units of the last significant digit are given in parentheses. The parameters without confidence intervals were fixed during the fitting.

Table 3. Resonance constants of vibrational states of the first hexade of $H_2{}^{16}O$, in cm^{-1}

Anharmonic resonances

$V - V'$	F_k	$F_J \cdot 10$	$F_{xy} \cdot 10$	$F_{xyk} \cdot 10^3$
(021)–(101)	−0.279099(998)	−0.42715(675)	0.1974(187)	−0.5787(554)
(200)–(120)	−0.35876(398)	−0.4138(145)	0.2974(285)	−0.5622(840)
(002)–(120)	0.12628(540)	–	–	–
(002)–(200)	−0.33711(301)	1.2319(134)	0.4051(121)	−0.2418(325)
(040)–(120)	−0.52548(767)	−0.9426(254)	1.6199(244)	−2.0301(803)
(040)–(200)	0.03136(785)	–	–	–

Coriolis coupling

$V - V'$	C_y	C_{xz}	C_{xzk}	C_{xzJ}	C_{xzkJ}
(120)–(101)	−1.1637(478)	−0.02837(399)	–	–	–
(120)–(021)	–	−0.311282(673)	–	–	–
(200)–(101)	–	−0.586353(652)	–	–	–
(200)–(021)	0.56348(657)	–	–	–	–
(002)–(101)	–	−0.278679(828)	–	$0.25994(762) \cdot 10^{-3}$	–
(002)–(021)	1.5421(604)	−0.06088(352)	–	–	–
(040)–(021)	−2.5806(252)	–	$-1.957(206) \cdot 10^{-3}$	–	$-0.1028(152) \cdot 10^{-4}$

See Note to Table 2.

3. Determination of parameters of the transformed transition (dipole) moment operator of the $H_2{}^{16}O$ molecule

The wave functions obtained from the solution of the inverse problem for levels were then used to simulate the experimental intensities of RV lines of the $H_2{}^{16}O$ molecule. The $a \to b$ transition intensities were calculated by the well-known equation[9]:

$$S_{ab} = \frac{8\pi^3 n\nu_{ab}}{3hc}\left[1-\exp\left(-\frac{hc}{kT}\nu_{ab}\right)\right]\frac{g_a}{Z(T)}\times$$
$$\times\exp\left(-\frac{hc}{kT}E_a\right)\left|\langle\Psi_a|M_z|\Psi_b\rangle\right|^2, \qquad (4)$$

where n is the gas density; ν_{ab} is the frequency of transition; g_a is the nuclear statistical weight of the lower level; E_a is the upper energy level; $Z(T)$ is the partition function; M_z is the transformed dipole moment operator; $|\Psi_a\rangle, |\Psi_b\rangle$ are wave functions of the levels a and b.

The transformed dipole moment operator can be represented as[9]:

$$M_z = \sum_{V\in\Gamma}|0\rangle\sum_k {}^V\mu'_k\,{}^VA_k\langle V|, \qquad (5)$$

where $\Gamma = \{(101), (021), (120), (200), (002), (040)\}$; ${}^V\mu'_1$ are the parameters to be determined; ${}^VA_k$ are rotational operators (Table 4).

To determine the parameters of the dipole moment, we used the measured intensities of 3557 lines.[1] In the course of fitting, some lines were excluded because of the large deviations from the calculation. Most of the excluded lines were determined with relatively large errors in Ref. 1. Finally, 3038 experimental levels were used to find 42 dipole moment parameters, which are summarized in Table 4.

The relative signs of the dipole moment parameters were determined quite reliably because of the strong resonance mixing of wave functions of different vibrational states. It should be noted that the intensities of the strongly resonating lines are in a satisfactory agreement with the measurements. This confirms the correct choice of the signs for the dipole moment parameters. The sign of ${}^{101}\mu'_1$ for the $\nu_1 + \nu_3$ band (most intense) was taken negative in accordance with the results of Ref. 10.

Table 4. Parameters of the dipole moment operator (in D) for the 2ν polyad

k	${}^{V}A_k$	(101)	(021)
1	φ_z	$-0.0131473(230)$	$-3.67961(880)\cdot 10^{-3}$
2	$\{\varphi_z, J^2\}$	$-0.1088(120)\cdot 10^{-5}$	$0.5163(630)\cdot 10^{-6}$
3	$\{\varphi_z, J_z^2\}$	$0.9072(380)\cdot 10^{-5}$	
4	$\frac{1}{2}\{\varphi_x, iJ_y\} - \frac{1}{2}\{i\varphi_y, J_x\}$	$0.10475(180)\cdot 10^{-3}$	$0.29667(810)\cdot 10^{-4}$
5	$\frac{1}{2}\{\varphi_x, \{J_x, J_z\}\} - \frac{1}{2}\{\varphi_y, \{J_y, J_z\}\}$		
6	$\frac{1}{2}\{\varphi_x, iJ_y\} + \frac{1}{2}\{i\varphi_y, J_x\}$	$-0.57721(540)\cdot 10^{-4}$	$-0.30261(260)\cdot 10^{-4}$
7	$\frac{1}{2}\{\varphi_x, \{J_x, J_z\}\} + \frac{1}{2}\{i\varphi_y, \{J_z, J_y\}\}$	$0.9609(600)\cdot 10^{-6}$	$0.18676(340)\cdot 10^{-5}$
8	$\{\varphi_z, J_{xy}^2\}$	$-0.8250(680)\cdot 10^{-6}$	$-0.6766(280)\cdot 10^{-6}$
	Number of lines in fitting	782	617
	RMS deviation, %	4.48	5.37

k	${}^{V}A_k$	(120)	(200)	(002)	(040)
1	φ_x	$0.81534(190)\cdot 10^{-3}$	$4.86625(960)\cdot 10^{-3}$	$-0.82052(270)\cdot 10^{-3}$	$0.49092(350)\cdot 10^{-4}$
2	$\{\varphi_x, J^2\}$		$-0.5485(680)\cdot 10^{-6}$	$-0.10436(230)\cdot 10^{-5}$	
3	$\{\varphi_x, J_z^2\}$	$-0.8846(830)\cdot 10^{-6}$	$0.635(170)\cdot 10^{-6}$	$0.17591(830)\cdot 10^{-5}$	$0.11074(320)\cdot 10^{-5}$
4	$\{i\varphi_y, J_z\}$	$-0.22920(250)\cdot 10^{-4}$	$-1.15700(690)\cdot 10^{-4}$	$-0.25379(330)\cdot 10^{-4}$	$0.22948(640)\cdot 10^{-5}$
5	$\{\varphi_z, iJ_y\}$	$-0.1494(150)\cdot 10^{-5}$	$0.39227(550)\cdot 10^{-4}$	$-0.60088(220)\cdot 10^{-4}$	$0.47399(440)\cdot 10^{-5}$
6	$\{\varphi_z, \{J_x, J_z\}\}$	$-0.2160(320)\cdot 10^{-6}$	$0.3443(610)\cdot 10^{-6}$	$0.4678(360)\cdot 10^{-6}$	$-0.4809(150)\cdot 10^{-6}$
7	$\frac{1}{2}\{\varphi_z, J_{xy}^2\} - \frac{1}{2}\{\varphi_z, \{J_x, J_y\}\}$	$0.3063(300)\cdot 10^{-6}$	$-0.7417(910)\cdot 10^{-6}$	$-0.2480(360)\cdot 10^{-6}$	
8	$\frac{1}{2}\{\varphi_z, J_{xy}^2\} + \frac{1}{2}\{\varphi_z, \{J_x, J_y\}\}$	$0.5115(290)\cdot 10^{-6}$	$0.4114(310)\cdot 10^{-6}$	$-0.3949(220)\cdot 10^{-6}$	$0.1201(140)\cdot 10^{-6}$
	Number of lines in fitting	383	631	479	146
	RMS deviation, %	4.87	4.25	5.00	7.00

See Note to Table 2.

The isotopic substitution of oxygen only slightly changes the spectroscopic parameters because of a relatively small change of mass. On the other hand, the mixing among the parameters ${}^{V}\mu_1'$ of different bands following the condition $F_0 = 0$ for anharmonic resonances leads to only slight decrease of these parameters for more intense bands, whereas for weaker bands such a mixing can lead to alternation of the sign of parameters. For these reasons, the signs of the parameters ${}^{V}\mu_1'$, obtained in this paper, differ from those in Ref. 10. Having tested different combinations of signs, we found that the set given in Table 4 is the best.

The rms error of calculation of the intensities was 4.86%, which corresponds to the average experimental uncertainty. The integral intensities of the $H_2{}^{16}O$ bands, calculated as a sum of all calculated lines having the intensity higher than 10^{-7} cm$^{-2}\cdot$atm^{-1}, are tabulated below.

Band	Integral intensity, cm$^{-2}\cdot$atm^{-1}	Band	Integral intensity, cm$^{-2}\cdot$atm^{-1}
$\nu_1 + \nu_3$	12.402	$2\nu_1$	1.839
$2\nu_2 + \nu_3$	0.997	$2\nu_3$	0.0952
$\nu_1 + 2\nu_2$	0.0627	$4\nu_2$	0.0024

Figure 1 compares the experimental spectrum from Ref. 1 (top), the calculated spectrum obtained in this work (bottom), and the Partridge and Schwenke data[3] (center). It can be seen that all the three plots are in a good agreement.

4. Results and discussion

The resonance interactions between the terms of the first hexade are very strong, which manifests itself in the existence of the so-called inversion, when the resonance perturbation changes the ordinary order of levels, determined by the rigid top model. Note, as an example, the inverted rotational levels [955] and [954] of the vibrational state (120), [808] and [818] of the state (002), and [955] and [954] of the state (200), where the inversion can be as large as 3 cm^{-1}. In some cases, the mixing of the basis wave functions is very significant and gives the mixing coefficients close to 50%. The level [955] (200) has almost equal contributions (45.8 and 45.6%) coming from the vibrational states (200) and (002), respectively. In such cases, the assignment of quantum numbers becomes quite conditional. We assigned levels by the main contributor to their wave functions, as was proposed by Kwan.[11]

The resonance interactions in the hexade often involve several vibrational states. For example, four levels with $J > 9$ and $K_a = 8$, 9 of the vibrational state (101) have practically identical mixing with the vibrational state (002), $K_a = 7$, 8. At the same time, both sets of the levels interact with the corresponding levels of the vibrational state (021) through the Fermi and Coriolis resonances (mixing coefficients of 10 to 20%). To completely take the complex resonance couplings into account, we had to include the high-order resonance constants: F_{xyk}, C_{xzk}, C_{xzkJ} and others, into the fitting (see Table 3).

Figure 2 shows the contributions of resonance effects to the dependences on the rotational quantum number J. They are determined as

$$m_v(J) = \sum_{V' \neq V} \sum_{K_a K_c} S_{V'}^{VJK_aK_c} / (2J+1), \quad (6)$$

where $S_{V'}^{VJK_aK_c}$ are the mixing coefficients of the wave function. It can be seen that the resonance effects increase sharply at $J = 8$ and become decisive at $J > 10$.

The high-excited state (040) can be considered as isolated up to $J = 4$. However, starting from $J = 5$, some levels of (040) fall in resonance with the states (021), (120), and (200). Due to the resonance intensity re-distribution, leading to the growth of the intensity of the weak component of the pair being in resonance, we managed to assign the transitions to the high-excited energy levels of the state (040) with $K_a = 4$ and 5: [550], [651], [752], [854], [945], and [1056]. The new levels were determined by the combination differences from 2–5 lines, and the agreement between the experimental and calculated line positions was, as a rule, very good. The mixing between these levels and the levels of (021), (120), and (200) varies from 3 to 30%. This manifests itself in relatively high intensities of the corresponding transitions to the levels of (040), up to $5.81 \cdot 10^4$ cm$^{-2} \cdot$ atm^{-1}. In spite of the presence of good combination differences, the major part of the transitions to high-excited levels of the state (040) remained unassigned or was assigned in Ref. 1 incorrectly.

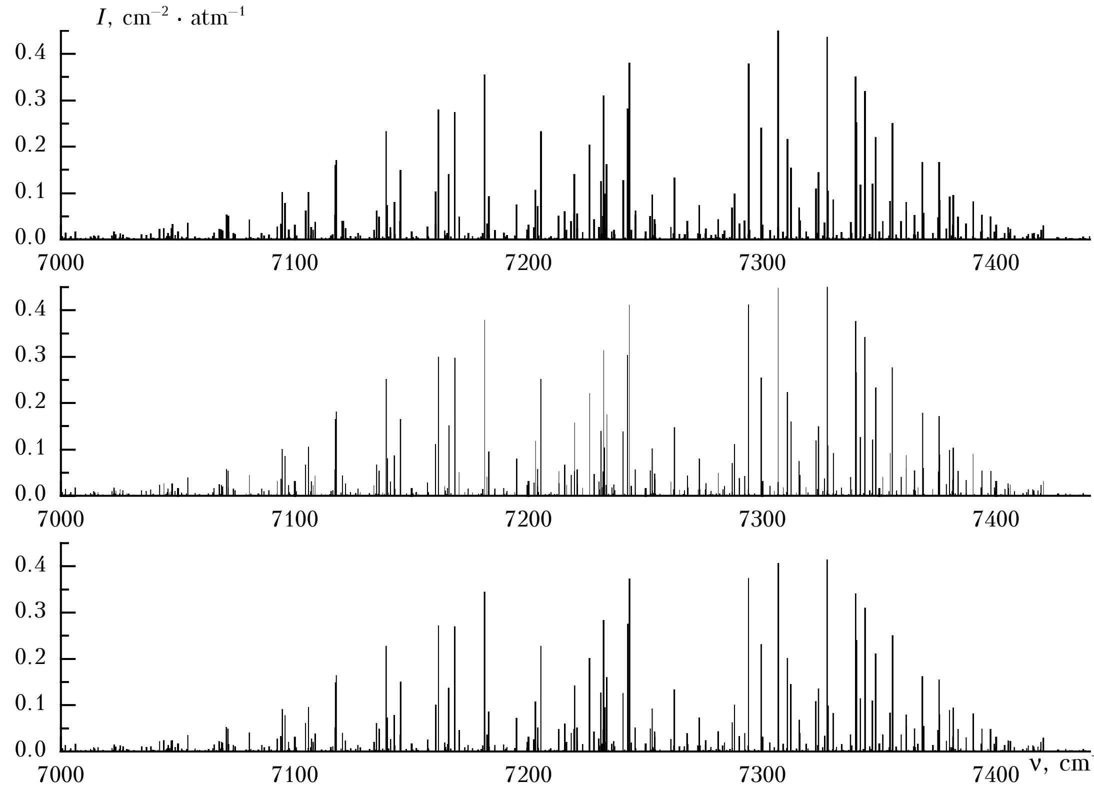

Fig. 1.

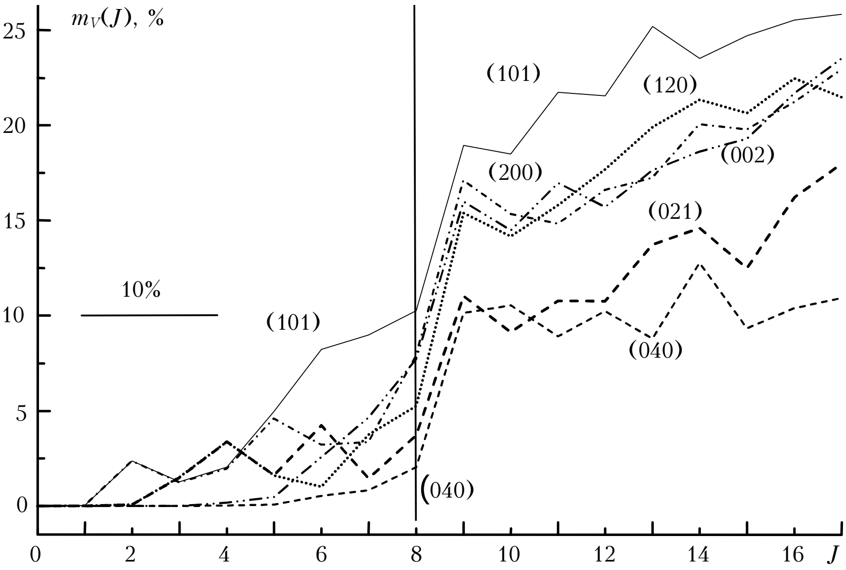

Fig. 2.

Owing to the strong centrifugal distortion, the consideration of resonance interactions between the high-excited bending states (021), (120), and (040) proved to be the most complicated, which resulted in the worst reconstruction of the energy levels for these states among all terms of the hexade.

It is also interesting to compare the results of fitting the $H_2{}^{16}O$ energy levels, carried out in this work, to the data from Ref. 4. In Ref. 4, the method of generating functions provided for a much better reconstruction of the energy levels for the first hexade (0.014 cm^{-1}) than in this work (0.025 cm^{-1}). However, the number of levels included in the fitting in Ref. 4 (749) was much smaller than in our work (858), while the difficulty of solution of the inverse problem is directly proportional to the number of levels included in the fitting. Keeping this circumstance in mind, the rms deviation of 0.025 cm^{-1} achieved in our work seems to be quite satisfactory. An advantage of our work is that the inverse problem for energy levels was solved in parallel with the simulation of intensities of RV lines and new assignment of the spectrum in the region under study.

As was repeatedly mentioned in the literature, the quality of simulation of the experimental intensities strongly depends on the coefficients of mixing of wave functions and, consequently, on the scheme of resonance couplings used in the calculation of energy levels. Although we have managed to reconstruct the measured intensities of the transitions in the region of the first hexade with the mean accuracy close to the experimental one, the calculated intensities of some strongly perturbed transitions remained significantly distorted. Thus, the calculated intensity of the transitions to the level [651] of the state (040), perturbed by the resonance with stronger transitions to the level [625] (021), is 30% lower than the experimental one. Such deviations take place for some other lines as well.

Reference 1 presents a great number of line intensities with the declared error of 15%, but it is noted that, in fact, 15% can mean the error up to 60%. Our calculation, as well as the data from Ref. 3, suggested that the true error could be as high as three orders of magnitude. In Ref. 1, there are also some misprints in both line positions and intensities. Table 5 exemplifies the incorrect intensities from Ref. 1.

It is interesting to note the appearance of local interpolyad (HEL) resonance[12] between the states (002) and (050), which leads to intensification of weak transitions to the levels [414] and [505] (050), which were assigned in the spectrum.

Conclusions

Using the Padé–Borel approximants and considering high-order resonance interactions, we obtained the spectroscopic parameters, reconstructed the positions and intensities of lines belonging to the first hexade of $H_2{}^{16}O$ vibrational states with the accuracy sufficient for unambiguous and exact assignment of the absorption spectrum in the 5750–7965 cm^{-1} region.

The fitting of energy levels by the method of effective Hamiltonian is complicated due to the resonance interaction, which becomes too complicated for high-excited RV states. A more reliable model of the operators of resonance interactions should likely be used in place of the simple expansion (2) and (3).

The set of parameters of the transformed dipole moment operator, obtained in this paper, can be used for reconstruction of the dipole moment function of the H_2O molecule within the framework of the approach developed in Ref. 13.

The presence of two independent precision calculations of the intensities of RV lines (calculation made in this work within the framework of the effective Hamiltonian method and the *ab initio*

Table 5. Example of incorrect experimental intensities from Ref. 1

ν, cm^{-1}	I_{exp}	I_{our}	I [Ref.3]	$V_1V_2V_3$	$J\ K_a\ K_c$ upper	$J\ K_a\ K_c$ lower
	cm^{-2}·atm^{-1}					
5985.7342	$1.01\cdot10^{-6}$	$1.0\cdot10^{-5}$	$1.2\cdot10^{-5}$	040	7 0 7	8 1 8
6701.0744	$1.34\cdot10^{-6}$	$1.3\cdot10^{-5}$	$1.5\cdot10^{-5}$	101	9 3 7	10 5 6
6773.1208	$9.93\cdot10^{-4}$	$9.8\cdot10^{-5}$	$1.1\cdot10^{-4}$	200	8 5 4	9 6 3
6785.1919	$4.90\cdot10^{-7}$	$1.1\cdot10^{-5}$	$1.3\cdot10^{-5}$	002	8 3 6	9 6 3
6795.2500	$2.90\cdot10^{-6}$	$2.7\cdot10^{-7}$	$3.8\cdot10^{-7}$	200	8 1 8	8 4 5
6957.4715	$1.38\cdot10^{-2}$	$1.4\cdot10^{-3}$	$1.6\cdot10^{-3}$	101	3 2 2	4 4 1
7028.7530	$2.00\cdot10^{-5}$	$5.6\cdot10^{-7}$	$5.6\cdot10^{-7}$	101	9 3 6	9 5 5
7104.5410	$1.00\cdot10^{-5}$	$3.6\cdot10^{-7}$	$3.2\cdot10^{-7}$	200	9 1 9	8 2 6
7116.9350	$2.00\cdot10^{-4}$	$3.7\cdot10^{-5}$	$4.4\cdot10^{-5}$	021	5 2 3	4 0 4
7116.9950	$3.00\cdot10^{-5}$	$3.0\cdot10^{-7}$	$6.7\cdot10^{-7}$	200	7 0 7	6 3 4
7123.7790	$8.67\cdot10^{-5}$	$3.2\cdot10^{-6}$	$1.7\cdot10^{-6}$	200	7 1 6	6 4 3
7127.7380	$1.00\cdot10^{-5}$	$1.3\cdot10^{-6}$	$1.7\cdot10^{-6}$	200	6 0 6	5 3 3
7131.9000	$2.25\cdot10^{-5}$	$2.3\cdot10^{-7}$	$5.1\cdot10^{-7}$	101	9 1 9	8 3 6
7164.6260	$9.90\cdot10^{-6}$	$3.4\cdot10^{-5}$	$3.9\cdot10^{-5}$	101	9 3 7	8 5 4
7168.9190	$2.40\cdot10^{-5}$	$8.4\cdot10^{-7}$	$1.3\cdot10^{-6}$	101	9 2 8	8 4 5
7174.1250	$5.00\cdot10^{-5}$	$2.4\cdot10^{-4}$	$2.8\cdot10^{-4}$	002	5 3 2	6 4 3
7180.3230	$3.00\cdot10^{-4}$	$8.6\cdot10^{-6}$	$9.3\cdot10^{-6}$	002	10 6 5	10 7 4
7194.1930	$2.50\cdot10^{-4}$	$2.0\cdot10^{-5}$	$2.7\cdot10^{-5}$	021	5 3 3	4 1 4
7202.3260	$1.50\cdot10^{-4}$	$2.3\cdot10^{-5}$	$2.9\cdot10^{-5}$	200	5 3 2	4 4 1
7207.9950	$3.00\cdot10^{-5}$	$1.7\cdot10^{-7}$	$6.6\cdot10^{-8}$	200	7 4 3	6 5 2
7211.5989	$2.35\cdot10^{-5}$	$2.4\cdot10^{-4}$	$2.6\cdot10^{-4}$	021	8 6 2	7 6 1
7232.3202	$1.00\cdot10^{-5}$	$1.8\cdot10^{-4}$	$1.9\cdot10^{-4}$	002	6 5 2	6 6 1
7232.3830	$3.30\cdot10^{-6}$	$5.9\cdot10^{-5}$	$6.4\cdot10^{-5}$	002	6 5 1	6 6 0
7236.5870	$2.00\cdot10^{-5}$	$3.3\cdot10^{-7}$	$1.1\cdot10^{-6}$	021	6 3 4	5 1 5
7240.7470	$2.00\cdot10^{-5}$	$3.0\cdot10^{-6}$	$4.3\cdot10^{-6}$	021	5 4 1	4 2 2
7242.8560	$1.00\cdot10^{-4}$	$3.7\cdot10^{-4}$	$4.2\cdot10^{-4}$	200	4 3 2	5 0 5
7245.7197	$6.15\cdot10^{-2}$	$6.9\cdot10^{-3}$	$7.8\cdot10^{-3}$	200	4 1 3	4 0 4
7261.2080	$3.00\cdot10^{-5}$	$3.9\cdot10^{-7}$	$4.2\cdot10^{-7}$	101	4 4 0	5 2 3
7279.9144	$3.47\cdot10^{-3}$	$6.1\cdot10^{-6}$	$6.5\cdot10^{-6}$	120	7 6 2	6 5 1
7279.9504	$9.88\cdot10^{-3}$	$1.8\cdot10^{-5}$	$1.9\cdot10^{-5}$	120	7 6 1	6 5 2
7294.4850	$2.00\cdot10^{-2}$	$3.3\cdot10^{-5}$	$2.0\cdot10^{-5}$	200	2 2 0	1 1 1
7348.5510	$1.00\cdot10^{-6}$	$1.7\cdot10^{-5}$	$1.9\cdot10^{-5}$	120	6 5 2	5 2 3
		$3.3\cdot10^{-5}$	$3.7\cdot10^{-5}$	002	8 0 8	7 3 5
7361.7722	$3.00\cdot10^{-6}$	$5.9\cdot10^{-5}$	$6.2\cdot10^{-5}$	021	9 4 6	9 0 9
7365.0860	$1.00\cdot10^{-4}$	$1.1\cdot10^{-3}$	$1.3\cdot10^{-3}$	200	5 3 2	5 0 5
7390.0720	$6.00\cdot10^{-3}$	$4.1\cdot10^{-5}$	$4.7\cdot10^{-5}$	200	4 4 0	4 1 3
		$2.2\cdot10^{-4}$	$3.1\cdot10^{-4}$	200	5 3 2	4 2 3
7426.4090	$3.00\cdot10^{-5}$	$2.8\cdot10^{-6}$	$3.0\cdot10^{-6}$	101	6 5 2	6 3 3
7476.6820	$5.00\cdot10^{-6}$	$2.3\cdot10^{-5}$	$2.4\cdot10^{-5}$	021	7 6 2	6 4 3

calculation from Ref. 3) allowed us to perform the critical analysis of the quality of experimental intensities recorded in Ref. 1. As a result, we have obtained the detailed and accurate absorption spectrum of the water vapor molecule in the region of 5750–7965 cm^{-1}.

Acknowledgments

The authors are grateful to Professors P. Bernath and V.I. Starikov for useful discussions.

This work was supported, in part, by the Russian Foundation for Basic Research (Grants No. 02–07–90139v and No. 02–03–32512), INTAS (Grant No. 03–51–3394), and the Scientific School by Prof. S.D. Tvorogov (Grant No. 2.10).

References

1. R.A. Toth, Appl. Opt. **33**, No. 21, 4851–4867 (1994).
2. P. Macko, D. Romanini, S. Mikhailenko, O. Naumenko, S. Kassi, A. Jenouvrier, Vl. Tyuterev, and A. Campargue, J. Mol. Spectrosc. **227**, Issue 1, 90–108 (2004).
3. H. Partridge and D. Schwenke, J. Chem. Phys. **106**, No. 11, 4618–4639 (1997).
4. V.I. Starikov and S.N. Mikhailenko, J. Mol. Struct. **442**, 39–53 (1998).
5. A.D. Bykov, O.V. Naumenko, A.M. Pshenichnikov, L.N. Sinitsa, and A.P. Shcherbakov, Opt. Spektrosk. **94**, No. 3, 528–537 (2003).
6. R.A. Toth, J. Opt. Soc. Am. B **8**, 2236–2255 (1991).
7. J. Tennyson, N.F. Zobov, R. Williamson, O.L. Polyansky, and P.F. Bernath, J. Phys. Chem. Ref. Data **30**, No. 3, 735–831 (2001).
8. O.L. Polyansky, J. Mol. Spectrosc. **112**, No. 1, 79–87 (1985).
9. J.-M. Flaud and C. Camy-Peyret, J. Mol. Spectrosc. **55**, 278–310 (1975).
10. O.N. Ulenikov and A.S. Zhilyakov, J. Mol. Spectrosc. **133**, No. 1, 1–9 (1989).
11. Y.Y. Kwan, J. Mol. Spectrosc. **71**, 260–280 (1978).
12. A.D. Bykov, O.V. Naumenko, L.N. Sinitsa, B.A. Voronin, J.-M. Fluad, C. Camy-Peyret, and R. Lanquetin, J. Mol. Spectrosc. **205**, No. 1, 1–8 (2001).
13. O.N. Sulakshina, Yu. Borkov, A. Barbe, and Vl.G. Tyuterev, in: *IRS2000: Current Problems in Atmospheric Radiation* (A.Deepak Publishing, 2001), pp. 651–654.